ARMY RESEARCH LABORATORY

Wall-Based Registration of Two Scanning Ladar Sensors

by Gary A. Haas

ARL-TR-3595 **August 2005**

NOTICES

Disclaimers

The findings in this report are not to be construed as an official Department of the Army position unless so designated by other authorized documents.

Citation of manufacturer's or trade names does not constitute an official endorsement or approval of the use thereof.

DESTRUCTION NOTICE—Destroy this report when it is no longer needed. Do not return it to the originator.

Army Research Laboratory
Aberdeen Proving Ground, MD 21005-5066

ARL-TR-3595 **August 2005**

Wall-Based Registration of Two Scanning Ladar Sensors

Gary A. Haas
Weapons and Materials Research Directorate, ARL

REPORT DOCUMENTATION PAGE

Form Approved
OMB No. 0704-0188

1. REPORT DATE *(DD-MM-YYYY)*	2. REPORT TYPE	3. DATES COVERED (From - To)
August 2005	Final	October 2003 to February 2005

4. TITLE AND SUBTITLE

Wall-Based Registration of Two Scanning Ladar Sensors

5a. CONTRACT NUMBER

5b. GRANT NUMBER

5c. PROGRAM ELEMENT NUMBER

6. AUTHOR(S)

Gary A. Haas (ARL)

5d. PROJECT NUMBER
622618AH03

5e. TASK NUMBER

5f. WORK UNIT NUMBER

7. PERFORMING ORGANIZATION NAME(S) AND ADDRESS(ES)

U.S. Army Research Laboratory
Weapons and Materials Research Directorate
Aberdeen Proving Ground, MD 21005-5066

8. PERFORMING ORGANIZATION REPORT NUMBER
ARL-TR-3595

9. SPONSORING/MONITORING AGENCY NAME(S) AND ADDRESS(ES)

10. SPONSOR/MONITOR'S ACRONYM(S)

11. SPONSOR/MONITOR'S REPORT NUMBER(S)

12. DISTRIBUTION/AVAILABILITY STATEMENT

Approved for public release; distribution is unlimited.

13. SUPPLEMENTARY NOTES

14. ABSTRACT

This study evaluates the registration between a scanning ladar and a surveying ladar as a possible component in the registration of unmanned ground vehicle mobility sensors in the field. The structured scene used to generate registration data consists of the concave intersection of two walls and the flat pavement, effectively three orthogonal planes. The registration is formulated in terms of the parameters of the three planes. The extraction of the parameters from Cartesian point clouds produced by the ladars is described. The registration is generated and evaluated by qualitative techniques.

15. SUBJECT TERMS
ladar; registration; UGV

16. SECURITY CLASSIFICATION OF:			17. LIMITATION OF ABSTRACT	18. NUMBER OF PAGES	19a. NAME OF RESPONSIBLE PERSON
a. REPORT	b. ABSTRACT	c. THIS PAGE			Gary A. Haas
Unclassified	Unclassified	Unclassified	SAR	25	19b. TELEPHONE NUMBER (*Include area code*) 410-278-8867

Contents

List of Figures

1. Introduction

An autonomous unmanned ground vehicle (UGV) navigates unstructured terrain using sensors to detect and to classify its environs. Each sensor detects only a limited number of attributes of the world around it. The UGV perception subsystem must fuse the information from multiple sensors so that the traversability of terrain elements can be represented to the planning subsystem.

2. Registration

Integration or fusion of information from multiple sensors requires that the information be addressable in a common coordinate system. Sensors of interest to the UGV community, (e.g., imaging ladars and color cameras) generate information about the world in the coordinate system of the sensor. Although it is possible in principle to mechanically align the coordinate systems, in practice, precision alignment is not the rule. Fusion of information from sensors such as these requires the data to be converted to a common coordinate system in a process known as registration. In the domain of research UGVs, registration between two sensors is typically assumed to be time invariant and is performed off line at the time the sensors are installed on the UGV and perhaps periodically thereafter. The term "registration" refers to both the process of defining the mathematical transformation between sensor coordinate systems and the mathematical transformation itself.

A registration between a camera and a three-dimensional (3-D) point cloud from a ladar sensor is commonly computed from matching features in corresponding imagery produced by the two sensors (Elstrom, Smith, & Abidi, 1998). The imagery is frequently from a scene purposely designed for the registration, which provides features easily detected in the imagery from either sensor. A transformation is computed which consists of the rotation and translation that projects all 3-D point features into the corresponding two-dimensional (2-D) image features, minimizing some error term. This transformation is the mathematical transformation between the coordinate frames of the two sensors and is termed the registration transformation or, more commonly, the registration.

2.1 Sensors

The sensors of interest in this study are an imaging ladar manufactured by Schwartz Electro-Optics (SEO)[1] and a color video camera. The color camera is generic, producing 2-D color

[1] Design rights to this unit are now owned by General Dynamics Robotics Systems, Westminster, Maryland.

images at 640 by 480 pixels resolution. An 8-mm manual focus lens produces roughly a 45-degree field of view (FOV). Modeling and calibration are described in Oberle and Haas (2004).

The SEO ladar unit is rather unique in today's market in that it generates a 3-D image of its environment a number of times per second and so is capable of use on a moving vehicle as a geometric obstacle detector in an unstructured world. The 32-row by 180-column range image consists of 16 "facets" that comprise 4 rows by 90 columns of discrete elements called "rangels" (from "range pixel"). The facets shown in figure 1 tile the field of view of the range image, with a few rangels overlapping between corresponding left and right facets. Each rangel represents the range to something in the environment which has reflected enough energy to cross the detection threshold of the ladar detector. For each rangel, the direction is known in the coordinate frame of the sensor, so the magnitude and direction are converted to the more useful Cartesian form. The result is a cloud of 3-D Cartesian points in the local sensor coordinate frame. The FOV of the unit is 86 degrees horizontal by 20 degrees vertical; its angular resolution is 0.658 by 0.5 degree. See Shneier, Chang, Hong, Cheok, and Scott (2003) and Hong, Rasmussen, Chang, and Shneier (2002) for other details.

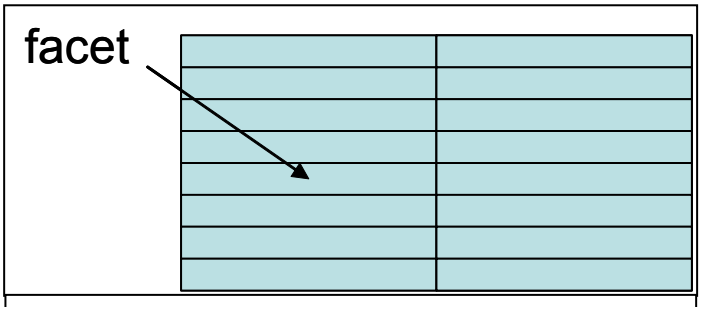

Figure 1. Facets tile to form image.

2.2 Composite Registration

For the data set described herein, the conventional approach to registration (e.g., matching point features) was deemed undesirable for the following reasons. First and foremost, point features are indistinct in the sparse SEO imagery. The intensity of a rangel return was not available from this unit, only the time-of-flight-based range. Thus, there is no reflectance-based image in which to look for features apparent in the camera image.

It is possible to produce a ladar-based image with the use of the two dimensions of the ladar "image plane" to define an image point and represent the third dimension as a "false" color. A well-silhouetted corner feature in ladar data presented in this fashion can be detected. However, the large mismatch in the angular resolution of the two sensors[2] limits the ability to localize the point correspondence.

[2]One ladar image point created in this fashion is approximately 50 times the size of a pixel from the camera image.

Third, the point features most readily distinguished in ladar imagery are well-silhouetted corners. However, any edge in a ladar image is subject to the "mixed pixel" effect (Tuley, Vandapel, & Hebert, 2004). This occurs when the ladar impinges on objects in the environment at different ranges, resulting in returns from each. The range reported is incorrect and is usually intermediate between the two correct ranges. An edge rangel is almost surely a mixed pixel, further reducing the certainty of location of the feature.

A final consideration was an interest in exploring a registration technique requiring less manual feature matching, a task not well suited to field operations and maintenance.

Instead, an approach was implemented, based on a variation of that described in (Shneier et al., 2003), with elements of the same sensor suite of the Shneier paper. Sensor data from the camera and the SEO ladar were separately registered to high-accuracy, high-resolution data from a Riegl[3] LMS-210 surveying ladar collected from the same registration scene. The registration between SEO ladar and camera was to be built from the registrations of the two sensors to the Riegl intermediary. The Riegl was used as an intermediate because the resolution is similar to that of the camera and because the Riegl produces not only a range at each data point but an intensity measure as well. The intensity of the reflectance at each point can be displayed in a manner that resembles a camera image, facilitating matching of features between the two sensors.

The structured registration scene shown in figure 2 consists of the concave intersection of two walls and the flat asphalt-covered ground. In the foreground are several planar targets on stanchions, including one target composed of surfaces and voids alternated in a checkerboard-like configuration. The poster-like targets provide corners evident in both the camera and Riegl reflectance images. The scene also contains the ground and two intersecting walls which provide planar features evident in data from the SEO and Riegl ladars. The registration between camera and Riegl ladar was calculated with conventional camera calibration methods that treated the 3-D feature locations from the Riegl sensor as a surrogate for ground truth of the corner features. The registration between Riegl and SEO ladars was approached in an unorthodox fashion, which comprises the focus of this report.

[3]Manufactured by Riegl, Horn, Austria.

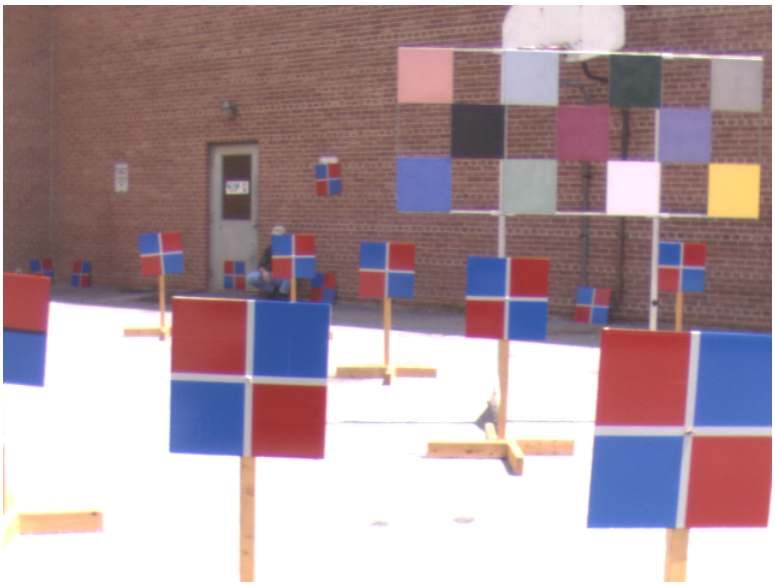

Figure 2. Registration scene with red/blue targets and multi-colored checkerboard target.

3. Three-Dimensional to Three-Dimensional Registration

Registration between the coarse SEO ladar and the high-resolution Riegl surveying ladar posed a new set of issues. The ICP (iterative closest or corresponding point) algorithm, currently the dominant method for 3-D-to-3-D registration (Rusinkiewicz & Levoy, 2001), was unfamiliar to the author at the onset of the effort, and disappointing early experiences with ICP (not herein documented) argued for a simpler approach. Instead, the author implemented a method based on the computation of the parameters defining the planes that correspond to the two walls and the ground in the registration scene and determined the rotation and translation between the two coordinate frames so defined. In general, good descriptions of surfaces can be extracted from ladar point clouds because a large number of data points support the small number of parameters describing a surface. In such an overdetermined system, the effect of a large error in an individual point can be expected to be overwhelmed by the large number of points without large error.

At the desired 10- to 20-meter range (the range of greatest interest in the intended use), the resolution of the SEO put only 30 or so points on the 0.5-m-square targets, with the edges subject to the "mixed pixel" effect. The corners were not clearly evident in the SEO image. The use of planar data from the targets was deemed un-promising. Only the planar data from the walls were used in the computation of the registration.

3.1 Wall-Based Method

The method is to extract from the ground and each of the two walls of the registration scene the equation describing the plane embedded therein. The vectors describing the orthogonal planes in one ladar's image are then rotated into the corresponding vectors in the other ladar's image to calculate the rotation and translation between the two images. The process of extracting the plane occurs in several steps. First, the SEO point cloud is rotated 180 degrees about the y axis to resolve axis-naming conventions between the ladars. The result is an approximate alignment between the two sensors. The pair of point clouds is then processed by means of software developed at Carnegie Mellon University, described in Vandapel, Donamukkala, and Hebert (2003), which separates points on the ground from others in the vegetation above the ground. A "ground" point has no points beneath it in the data set, while a "vegetation" (or "non-ground") point occurs above other points. For the flat terrain of the parking lot, the effect is to classify the walls and targets (imperfectly) as vegetation. The resulting "ground" is evaluated manually for outliers (tops of walls and posters erroneously classified as ground) and these points are removed by *ad hoc* methods. The remaining points are substantially planar, and these are submitted to a least squares planar fit, with points that deviate more than a few inches from the fit being culled. The remaining points are well described by the calculated plane and are judged to belong to the "ground" class.

The two walls are treated in a similar fashion. The entire point cloud is rotated so that the z axis in the new coordinate frame is approximately perpendicular to the surface of one of the walls. The rotated wall, which now has the characteristics required of "ground" by the ground extraction code, is isolated and extracted. Parameters of the ground plane are calculated and rotated back into the original coordinate frame. An example of a wall extracted in this fashion is depicted in figure 3.

3.2 Formulation

At this point in the process, the parameters of each wall (right, left, and ground[4]) have been calculated in the form

$$\underline{a}_{ws} * \underline{x}_{ws}' + b_{ws} = 0 \quad \text{where}$$

the notation $\underline{v}'$ indicates the transpose of vector (or matrix) $\underline{v}$;

$$\underline{a}_{ws} = [a1_{ws}\ a2_{ws}\ a3_{ws}], \text{ and } |\underline{a}_{ws}| = 1;$$

$a1_{ws}$, $a2_{ws}$, $a3_{ws}$, and b_{ws} are scalar;

the subscript w can assume the values {1, 2, 3} corresponding to {ground, right wall, left wall};

[4]We will hereafter refer to the ground as one of the walls defining the embedded coordinate frame. Hopefully, this will not be confusing, especially since we treated the walls as ground in the previous section.

the subscript s can assume the values {g, r} corresponding to {SEO or Riegl};

$\underline{x}_{ws}$ is of the form $[x\ y\ z]$,

and x, y, and z are the scalar coordinates of a data point from the w subset of the s sensor point cloud in local s sensor coordinate frame.

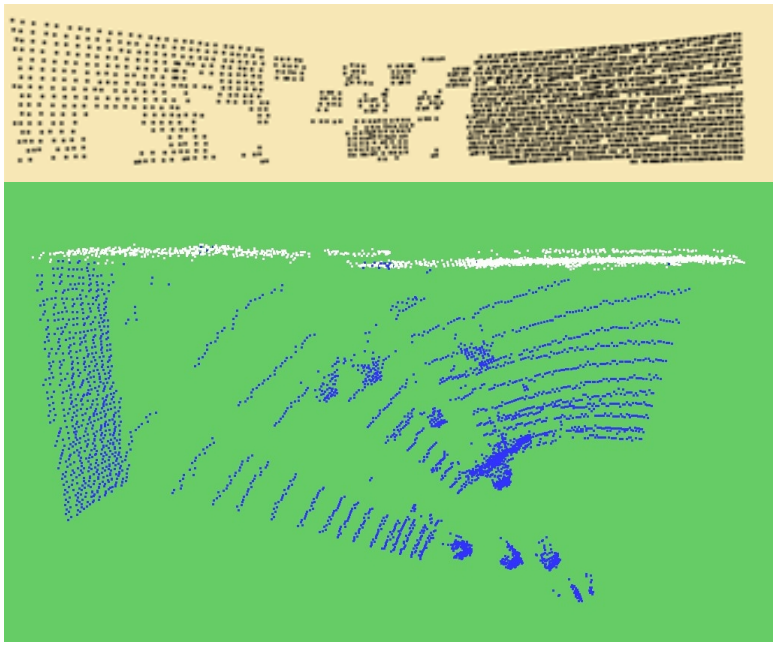

Figure 3. The right-hand wall isolated from the SEO data is shown in the top image. (Rectangular voids are occluded by posters in the foreground, which are eliminated as "non-ground" elements of the data. The wall is also shown in white in the lower image, rotated 90 degrees to plan view, along with points deemed non-ground, shown in blue. Planar targets can be seen as clusters of blue points in lower right of this image.)

Let us use these results to determine the rotation and translation between the coordinate frames of the two sensors.

First, we interpret the wall parameters. The unit vectors $\underline{a}_{1s}$, $\underline{a}_{2s}$, and $\underline{a}_{3s}$ are the perpendicular vectors to the three walls in the coordinate system of sensor s. They form the basis of a coordinate frame embedded in the walls of the scene, as seen by the sensor s. The origin of this embedded coordinate frame is the intersection of the three walls. We call the embedded coordinate frame "*e*." These basis vectors can be organized into a rotation matrix.

The rotation matrix $\underline{A}_s$, defined as

$$\underline{A}_s = \begin{bmatrix} \underline{a}_{1s} \\ \underline{a}_{2s} \\ \underline{a}_{3s} \end{bmatrix}' \quad \text{for } s = \{ g , r \},$$

rotates a point in the embedded coordinate frame to the coordinate frame of the s sensor.

The vector $\underline{b}_s = [b_{1s} \; b_{2s} \; b_{3s}]'$ is the origin of the sensor frame, measured in the embedded frame, and so represents the translation from the sensor coordinate frame to the embedded coordinate frame. A point $\underline{p}_e$ in the embedded coordinate frame can be mapped to the coordinate frame of sensor s by

$$\underline{p}_s = \underline{A}_s * \underline{p}_e - (\underline{A}_s * \underline{b}_s). \tag{1}$$

Now we compute the rotation $\underline{R}_{rg}$ and translation $\underline{t}_{rg}$ to transform a point in the coordinate frame of the g sensor to the coordinate frame of the r sensor.

The rotation $\underline{R}_{rg}$ between the coordinate frames of the two sensors can be calculated as the rotation between the orthogonal basis matrices $\underline{A}_g$ and $\underline{A}_r$,

$$\underline{R}_{rg} = \underline{A}_r * \text{inv}(\underline{A}_g) .$$

The translation between the sensor coordinate frames is somewhat more complex because the measured translations are defined in the embedded frame, not in either sensor frame. The translation between the coordinate frames of the two sensors is expressed as

$$\underline{t}_{rg} = (\underline{A}_r * (\underline{b}_g - \underline{b}_r)).$$

Intermediate steps in the development of this expression are documented in appendix A.

---

4. Metrics

4.1 Quantitative

Although there are several alternate ways of calculating the transformation between coordinate frames, there is no definitive quantitative measure of the correctness of the transformation. Rusinkiewicz and Levoy (2001) suggest a metric based on the sum of squared distances (SSD) from a point to the nearest surface. In this case, this could be implemented as the SSD from SEO

points to the corresponding Riegl plane. This measure was not implemented as part of this study but should be considered for any successor studies.

4.2 Visual Alignment

Qualitative measures are commonly used to assess the correctness of the transformation. One measure is inspection of the alignment of one point cloud transformed into the coordinate frame of the other. The mechanism used in this case is the Virtual Reality Modeling Language (VRML) visualization tool.[5] The SEO points were transformed to the Riegl frame with the registration calculated as described previously and were assigned a color (red). The Riegl points were assigned a different color (white), and both sets of points were viewed as part of the same VRML view (see figure 4). With built-in tools for moving the viewpoint around in the viewer, gross misalignment of the two point sets is apparent. Minor misalignments may escape scrutiny, however. One disadvantage is that the viewer has no cue to differentiate points in the foreground from points in the background, so features that cannot easily be silhouetted are difficult to assess. Another disadvantage is that the only depth cues come from moving the viewing perspective, so documenting phenomena for a presentation or paper is difficult. This method was used for initial assessment of the quality of 3-D-to-3-D registration.

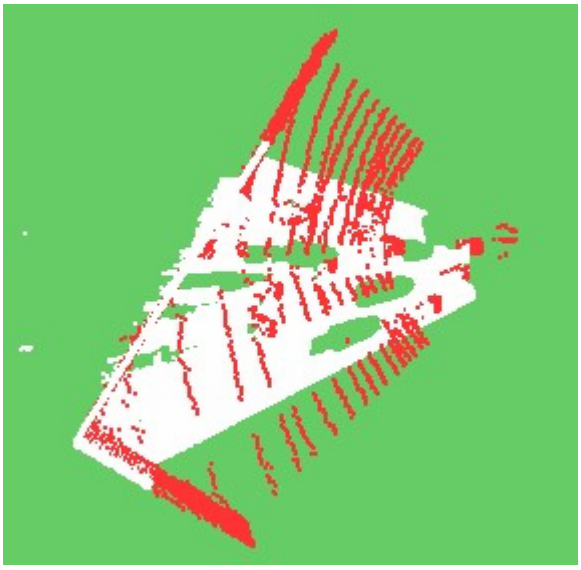

Figure 4. SEO data (in red) juxtaposed against Riegl data (in white) (plan view). (Note that the SEO FOV is wider than Riegl FOV.)

4.3 Project Points Into Image

A method for evaluating the quality of a 3-D-to-2-D registration is to project the 3-D points into the corresponding image[6]. A 3-D point is assigned the color of the pixel into which it projects

[5]I am indebted to Dr. Nicolas Vandapel for introducing me to this approach.

[6]I am indebted to Dr. Vandapel and Mr. Ranjith Unnakrishnan for suggesting this method.

and is viewed in a color VRML view. A high-quality registration is distinguished by appropriate color of the 3-D features in the view. This method was used to evaluate the end-to-end registration between camera and one or the other of the ladar sensors. It works reasonably well for high-resolution point clouds such as the Riegl. The low-resolution point clouds of the SEO were more difficult to assess. When the camera and ladar are far apart, points in the background frequently assume unexpected colors, since the sensors are occluded differently by features in the foreground. Only features in the foreground can be relied upon to display the color expected. An example of a good registration is shown in figure 5, which depicts the points from the Riegl ladar projected into the color camera image.

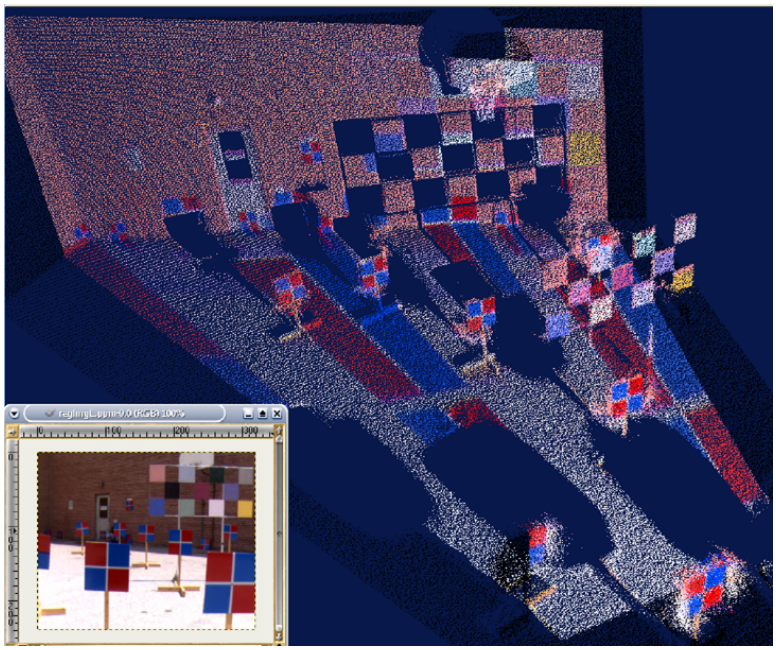

Figure 5. Visualization of registration of Riegl sensor data to color camera image at lower left. (The colors of the 3-D foreground posters match the image, as do un-occluded elements of the background [the door, for example], indicating a good registration.)

5. This Registration

The registration data were collected in May 2003 at the campus of the National Institute for Standards and Technology in Gaithersburg, Maryland.

The rotation between Riegl and SEO sensors was computed with the technique described herein. The equations describing the walls, as seen by the SEO sensor, were

$\underline{A}_r' =$

0.098932	0.0089963	0.99505
0.83984	-0.53779	-0.073874
0.53257	0.84365	-0.06791

$\underline{b}_s =$

2.2564
12.23
15.453

$\underline{A}_g' =$

0.099795	0.0049212	0.995
0.83659	-0.54593	-0.045581
0.55443	0.83099	-0.045497

$\underline{b}_s =$

0.74841
13.288
16.101

Note that in this form, the rows of the matrices are in the form of $\underline{a}_{ws}$. Since these $\underline{A}_s$ matrices are not quite orthogonal, they are brought into orthogonality by singular value decomposition (svd).

Next, the rotation between the sensor coordinate frames is computed. The rotation from the SEO coordinate frame to the Riegl coordinate frame is computed as

$\underline{R}_{rg} =$

0.99969	-0.017033	0.017899
0.016979	0.99985	0.0031528
-0.01795	-0.002848	0.99983

Finally, the translation from SEO to Riegl coordinate frames is computed:

$\underline{t}_{rg} =$

1.0851
-0.042551
-1.6228

The registration is evaluated first by an inspection of the alignment juxtaposing the registered data sets in a 3-D visualization (see figure 6). The alignment of the walls is substantially better than in figure 4. However, close inspection reveals that the alignment of the posters is poor (figure 7).

The registration is then evaluated by projection of the SEO points into the camera image, as was done in figure 3. The results, shown in figure 8, corroborate that the SEO sensor and camera are not well registered. In particular, there appears to be an offset of approximately 1 foot in the vertical direction. There is also an apparent discontinuity in the SEO data where the right and left facets merge. The calculated rotation between the two sensors appears correct.

Other anomalies were identified in the vicinity of the red and blue targets, which were constructed of retro-reflective material. The SEO sensor appears to detect these targets at a relatively shorter range than does the Riegl. The large multi-colored target, which is not retro-reflective, does not evidence this effect.

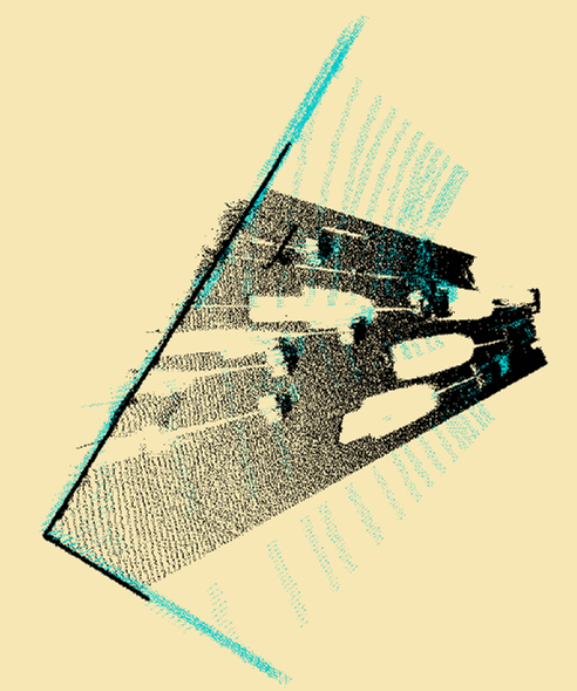

Figure 6. SEO data (in aqua) juxtaposed against Riegl data (in black) (plan view).

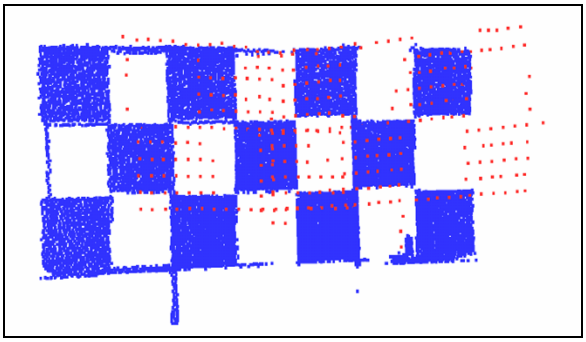

Figure 7. SEO data (red) for large poster juxtaposed with corresponding Riegl data (blue).

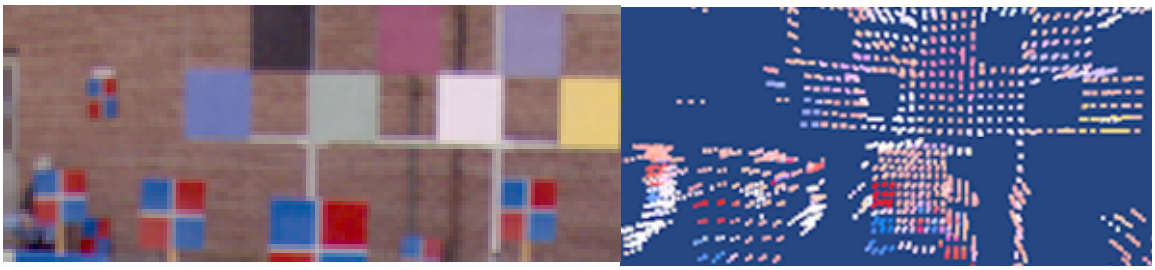

Figure 8. The colors assigned to the posters when the SEO data are projected into the camera image (right) do not align correctly with the colors and the boundaries of the camera image itself (left), indicating a poor registration between SEO sensor and camera.

6. Conclusions

The wall-based approach to aligning two imaging ladar sensors is an appealing notion. Upon sufficient reflection, the geometry is intuitive, and the mathematics to implement it are straightforward.

The benefit of such an approach is that walls in a mutually orthogonal configuration are available almost anywhere, so in principle, the ladar-to-wall portion of a UGV sensor alignment could be improvised in the field with a minimum of equipment and with relatively unsophisticated software. The wall-to-camera portion of the registration is required to complete the ladar-to-camera registration, which is the end-to-end result desired. Wall-to-camera registration without manual feature designation in such an improvised registration scene is left to another study.

However, this study did not result in a successful registration of the two sensors with this data set. The most likely source of error is the calibration of the SEO sensor used to convert the range image to a Cartesian point cloud. The calibration used in this study is based on a theoretical (rather than calibrated) set of direction vectors mapping the range image into a cloud of 3-D points. At least at the center where the two facets overlap, the calibration is suspect. A precise determination of the source of error is beyond the scope of this study.

The visualization tools used to evaluate the quality of the registration were inadequate, especially given the resolution of the SEO sensor. Having more than one (preferably at least three) corner point in the FOV would help quantify the effectiveness of the registration. It would also be helpful to increase the density of the SEO scan by slewing the sensor, although it increases the complexity of the sensor calibration.

7. References

Elstrom, M.; Smith, P.; Abidi, M. Stereo-based registration of LADAR and color imagery, SPIE Conference on Intelligent Robots and Computer Vision, 1998, pp. 343-354.

Hong, T.; Rasmussen, C.; Chang, T.; Shneier, M. Fusing Ladar and Color Image Information for Mobile Robot Feature Detection and Tracking. *Proceedings of the 7th International Conference on Intelligent Autonomous Systems*, Marina del Rey, CA, March 2002.

Oberle, W.; Haas, G. *LADAR-Camera Registration Using Object Pose and Camera Calibration Algorithms* ; ARL-TR-3147; U.S. Army Research Laboratory: Aberdeen Proving Ground, MD, April 2004.

Rusinkiewicz, S.; Levoy, M. Efficient Variants of the ICP Algorithm, Third International Conference on 3-D Digital Imaging and Modeling (3DIM '01), Quebec City, Canada, May 2001, p. 145.

Shneier, M.; Chang, T.; Hong, T.; Cheok, G.; Scott, H.S. A Repository of Sensor Data for Autonomous Driving Research, Proceedings of the SPIE Aerosense Conference. Orlando, FL, 2003.

Tuley, J.; Vandapel, N.; Hebert, M. Analysis and Removal of Artifacts in 3-D LADAR Data, IEEE International Conference on Robotics and Automation, 2005.

Vandapel, N.; Donamukkala, R.R.; Hebert, M. Quality Assessment of Traversability Maps From Aerial LIDAR Data for an Unmanned Ground Vehicle, International Conference on Intelligent Robots and Systems (IROS), October 2003.

INTENTIONALLY LEFT BLANK

Appendix A. Intermediate Steps in the Development of Expression for Transformation Between Coordinate Frames

From equation 1, for some sensor s, a point $\underline{p}_e$ in the embedded coordinate frame can be mapped to the coordinate frame of sensor s by

$$\underline{p}_s = \underline{A}_s * \underline{p}_e - (\underline{A}_s * \underline{b}_s). \quad (1)$$

Conversely,

$$\underline{p}_e = \text{inv}(\underline{A}_s) * \underline{p}_s + \underline{b}_s$$

Recall that $\underline{b}_s$ is a measure in the embedded frame *e*.

The point in coordinate frame s can be mapped to another coordinate frame t by

$$\begin{aligned}
\underline{p}_t &= \underline{A}_t * \underline{p}_e - (\underline{A}_t * \underline{b}_t) \\
&= \underline{A}_t * (\text{inv}(\underline{A}_s) * \underline{p}_s + \underline{b}_s) - (\underline{A}_t * \underline{b}_t) \\
&= \underline{A}_t * \text{inv}(\underline{A}_s) * \underline{p}_s + \underline{A}_t * \underline{b}_s - (\underline{A}_t * \underline{b}_t) \\
&= \underline{R}_{ts} * \underline{p}_s + (\underline{A}_t * (\underline{b}_s - \underline{b}_t)) \\
&= \underline{R}_{ts} * \underline{p}_s + \underline{t}_{ts}
\end{aligned}$$

So the translation $\underline{t}_{ts}$ from frame s to frame t is

$$\underline{t}_{ts} = (\underline{A}_t * (\underline{b}_s - \underline{b}_t))$$

and the rotation $\underline{R}_{ts}$ from frame s to frame t is

$$\underline{R}_{ts} = \underline{A}_t * \text{inv}(\underline{A}_s) .$$

NO. OF COPIES ORGANIZATION

* ADMINISTRATOR
DEFENSE TECHNICAL INFO CTR
ATTN DTIC OCA
8725 JOHN J KINGMAN RD STE 0944
FT BELVOIR VA 22060-6218
*pdf file only

1 DIRECTOR
US ARMY RSCH LABORATORY
ATTN IMNE ALC IMS MAIL & REC MGMT
2800 POWDER MILL RD
ADELPHI MD 20783-1197

1 DIRECTOR
US ARMY RSCH LABORATORY
ATTN AMSRD ARL CI OK TL TECH LIB
2800 POWDER MILL RD
ADELPHI MD 20783-1197

1 DIR OF COMBAT DEVELOPMENT
ATTN ATZK FD W MEINSHAUSEN
BLDG 1002 ROOM 326
1ST CAVALRY DIV RD
FT KNOX KY 40121-9142

1 CDR US TACOM-ARDEC
ATTN AMSTA AR FSS J WALSH
PICATINNY ARSENAL NJ 07806-5000

2 CDR TRADOC
ATTN ATINZA R REUSS
ATIN I C GREEN
BLDG 133
FT MONROE VA 23651

1 OFC OF THE SECY OF DEFENSE
CTR FOR COUNTERMEASURES
ATTN M A SCHUCK
WHITE SANDS MISSILE RANGE NM 88002-5519

2 CDR US ARMY ARMOR CTR & FT KNOX
ATTN TSM/ABRAMS COL D SZYDLOSKI
DIR UAMBL COL J HUGHES
FORT KNOX KY 40121

3 CDR US TACOM-ARDEC
ATTN AMSTA AR FSP G A PEZZANO
R SHORR
AMSTA AR FSP I R COLLETT
PICATINNY ARSENAL NJ 07806-5000

3 CDR US TACOM-ARDEC
ATTN AMSTA AR CCH A M PALTHINGAL
E LOGSDON M YOUNG
PICATINNY ARSENAL NJ 07806-5000

NO. OF COPIES ORGANIZATION

1 CDR US ARMY MMBL
ATTN J BURNS
BLDG 2021
BLACKHORSE REGIMENT DR
FT KNOX KY 40121

1 CDR ARMY RSCH OFC
4300 S MIAMI BLVD
RSCH TRIANGLE PK NC 27709

1 CDR US ARMY STRICOM
ATTN J STAHL
12350 RSCH PKWAY
ORLANDO FL 32826-3726

1 CDR US ARMY TRADOC
BATTLE LAB INTEGRATION & TECH DIR
ATTN ATCD B J A KLEVECZ
FT MONROE VA 23651-5850

1 OFC OF THE PROJECT MGR
MANEUVER AMMUNITION SYSTEMS
ATTN S BARRIERES
BLDG 354
PICATINNY ARSENAL NJ 07806-5000

1 CDR US ARMY TRADOC ANALYSIS CTR
ATTN ATRC WBA J GALLOWAY
WHITE SANDS MISSILE RANGE NM 88002

1 CDR USAAMC
DEPUTY G3 CURRENT OPERATIONS
ATTN N BIAMON
5001 EISENHOWER AVE
ALEXANDRIA VA 22333-0001

2 CDR US TACOM-ARDEC
ATTN AMSTA AR TD J HEDDERICK
B MADECK
PICATINNY ARSENAL NJ 07806-5000

2 CDR US TACOM-ARDEC
ATTN AMSTA AR TD J HEDDERICK
B MADECK
PICATINNY ARSENAL NJ 07806-5000

1 CDR USAARDEC
ATTN AMSRD AAR AE COL P JANKER
BLDG 94
PICATINNY, NJ 07806-5000

NO. OF
COPIES ORGANIZATION

1 PEO SOLDIER
ATTN C TAMEZ
5901 PUTNAM ROAD
BLDG 328
FT BELVOIR VA 22060-5422

ABERDEEN PROVING GROUND

1 DIRECTOR
US ARMY RSCH LABORATORY
ATTN AMSRD ARL CI OK (TECH LIB)
BLDG 4600

2 CDR US ARMY TECOM
ATTN AMSTE CD B SIMMONS
AMSTE CD M R COZBY
RYAN BLDG

4 DIR US AMSAA
ATTN AMXSY D D SHAEFFER/
W BROOKS
AMXSY CA G DRAKE/S FRANKLIN
APG MD 21005-5067

1 CDR US ATC
ATTN CSTE AEC COL BROWN
BLDG 400

2 DIRECTOR
US ARMY RSCH LABORATORY
ATTN AMSRD ARL WM J SMITH
T ROSENBERGER
BLDG 4600

1 DIRECTOR
US ARMY RSCH LABORATORY
ATTN AMSRD ARL WM B J MORRIS
BLDG 4600

2 DIRECTOR
US ARMY RSCH LABORATORY
ATTN AMSRD ARL WM BA D LYONS
AMSRD ARL WM BD B FORCH
BLDG 4600

1 DIRECTOR
US ARMY RSCH LABORATORY
ATTN AMSRD ARL WM BC P PLOSTINS
BLDG 390

NO. OF
COPIES ORGANIZATION

7 DIRECTOR
US ARMY RSCH LABORATORY
ATTN AMSRD ARL WM BF S WILKERSON/
R ANDERSON/P BUTLER/
C PATTERSON/J WALL/
M BARANOSKI/W OBERLE
BLDG 390

4 DIRECTOR
US ARMY RSCH LABORATORY
ATTN AMSRD ARL WM MB DOWDING
AMSRD ARL WM B VANLANDINGHAM
AMSRD ARL WM MC M MAHER
AMSRD ARL WM MD W ROY
AMSRD ARL WM MA S MCKNIGHT
BLDG 4600

3 DIRECTOR
US ARMY RSCH LABORATORY
ATTN AMSRD ARL WM T P BAKER
AMSRD ARL WM TC R COATES
AMSRD ARL WM TB R SKAGGS
BLDG 309

1 DIRECTOR
US ARMY RSCH LABORATORY
ATTN AMSRD ARL WM TD SCHOENFELD
BLDG 4600

1 DIRECTOR
US ARMY RSCH LABORATORY
ATTN AMSRD ARL WM TE B RINGERS
BLDG 1116A

1 DIRECTOR
US ARMY RSCH LABORATORY
ATTN AMSRD ARL WM T M ZOLTOSKI
BLDG 393